Electronic Supplementary Material (ESI) for New Journal of Chemistry.

A universal laser-assistant growth of transition metal nanoparticle on flexible graphene electrode for nonenzymatic glucose sensor

Wuyun Xie[2,3], Guang Yang, Mingqi Xu[2,3 *], and Xiangjie Bo[1, *]

[1]. Key Laboratory of Nanobiosensing and Nanobioanalysis at Universities of Jilin Province, Faculty of Chemistry, Northeast Normal University, Changchun, 130024, China

[2]. School of Physics, Northeast Normal University, Changchun, 130024, China

[3]. Jilin Province key Laboratory of the advanced energy development and the innovative application, Changchun 130024, China

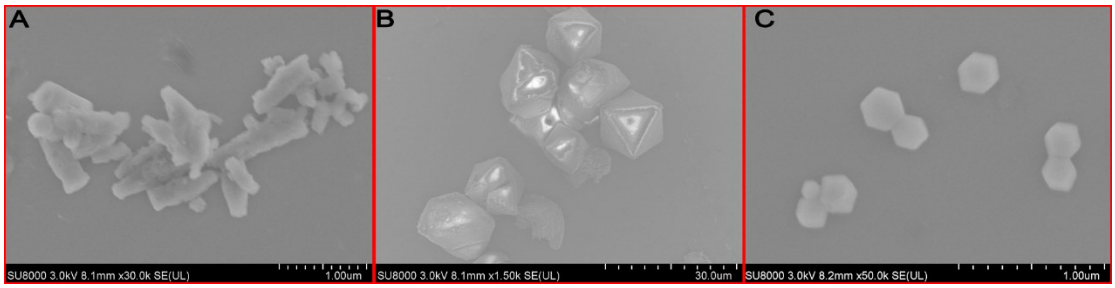

Figure S1 SEM images of Ni-MOFs, Cu-MOFs and Co-MOFs.

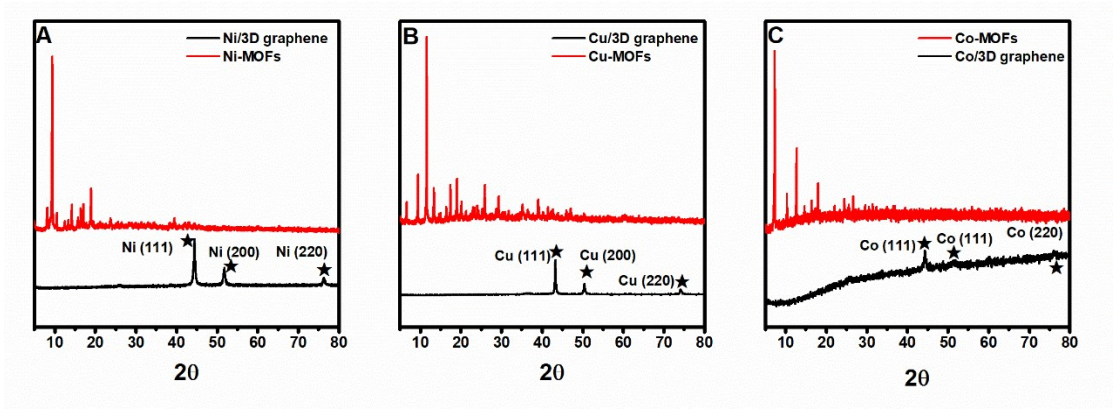

Figure S2 XRD patterns of (A) Ni-MOFs and their derived sample, (B) Cu-MOFs and their derived sample, (C) Co-MOFs and their derived sample.

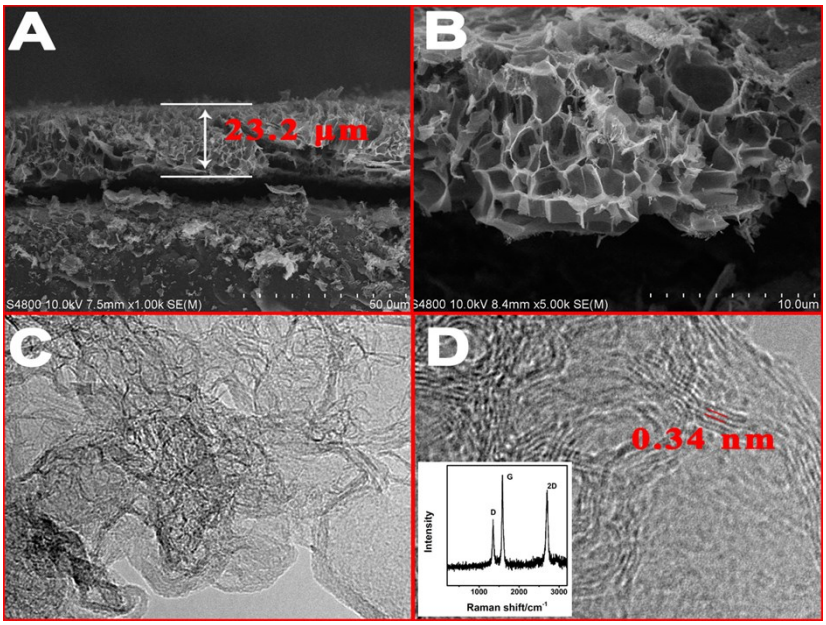

Figure S3 (A-B) SEM images of 3D GR. (C) TEM and (D) HRTEM images of 3D GR. Inset of (D): Raman spectrum of 3D GR.

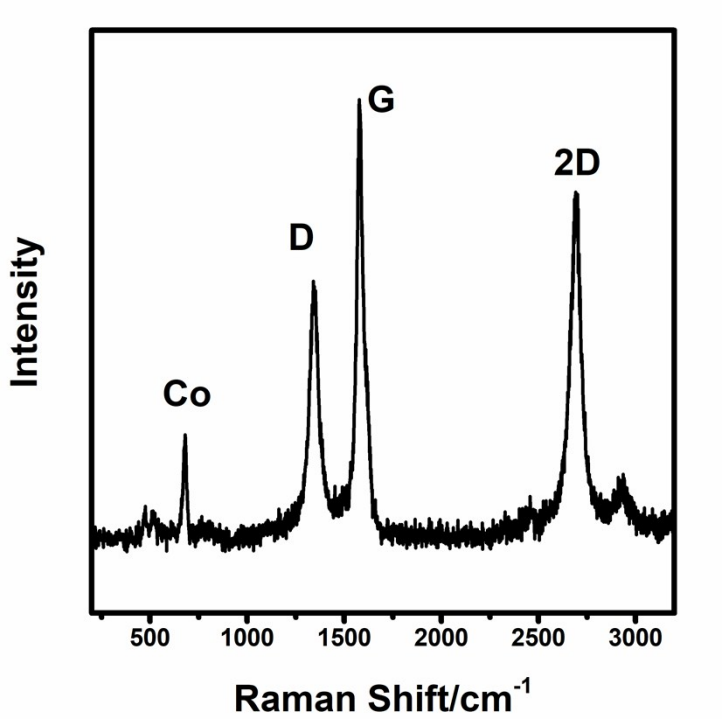

Figure S4 Raman spectrum of Co-MOFs-derived sample prepared by laser treatment of Co-MOFs on stainless steel.

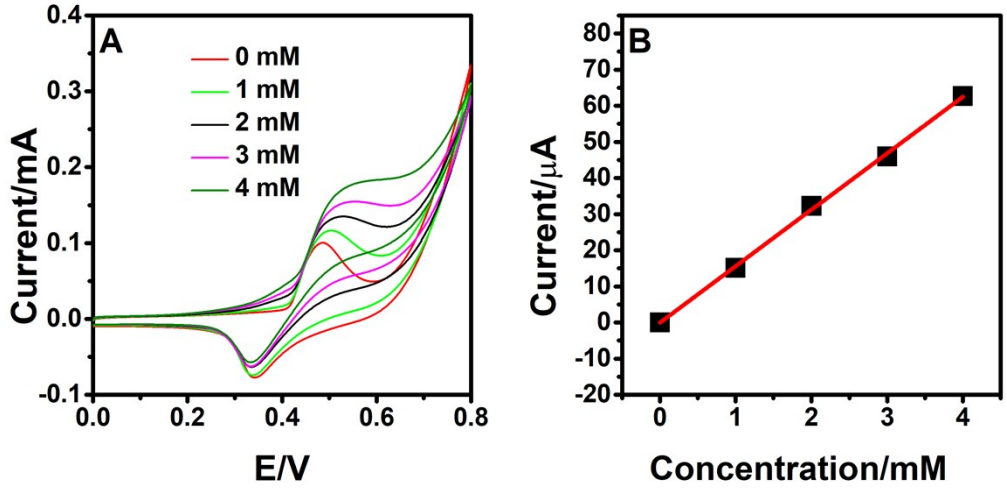

Figure S5 (A) CV responses of Ni/3D GR in 0.1 M NaOH containing different glucose. (E) The calibration curve of Ni/3D GR.

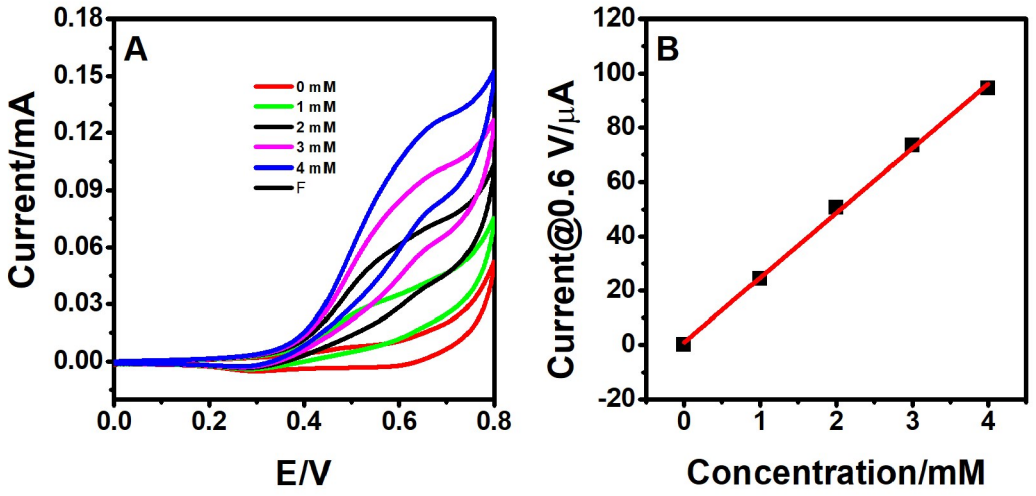

Figure S6 (A) CV responses of Cu/3D GR in 0.1 M NaOH containing different glucose. (E) The calibration curve of Cu/3D GR.

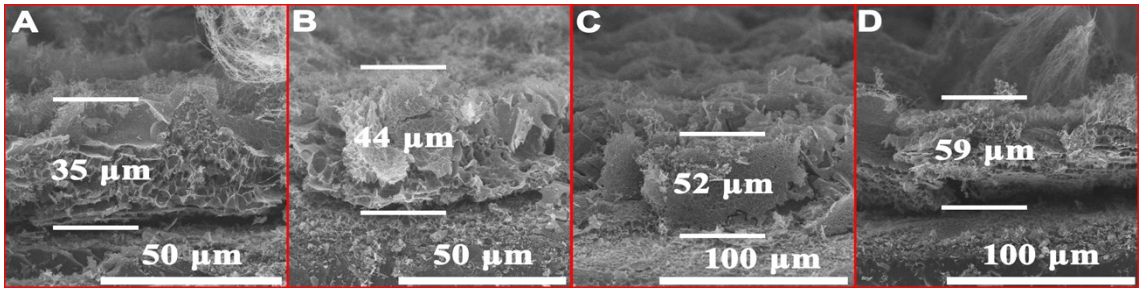

Figure S7 Cross-section SEM images of Co/3D GR with the precursor concentration of (A) 5 mg mL^{-1}, (B) 10 mg mL^{-1}, (C) 15 mg mL^{-1}, and (D) 20 mg mL^{-1}

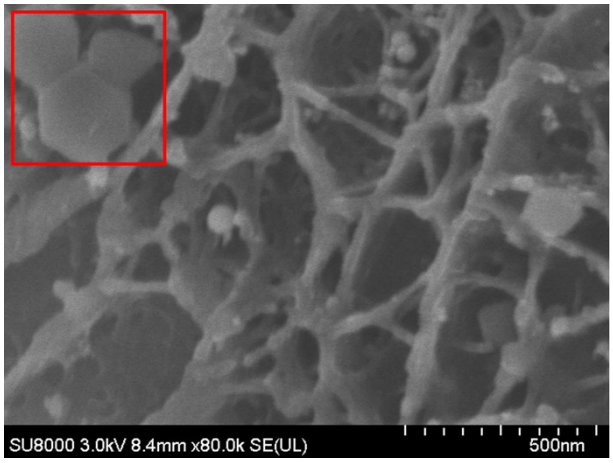

Figure S8 SEM image of Co/3D GR with the precursor concentration of 25 mg mL^{-1}.

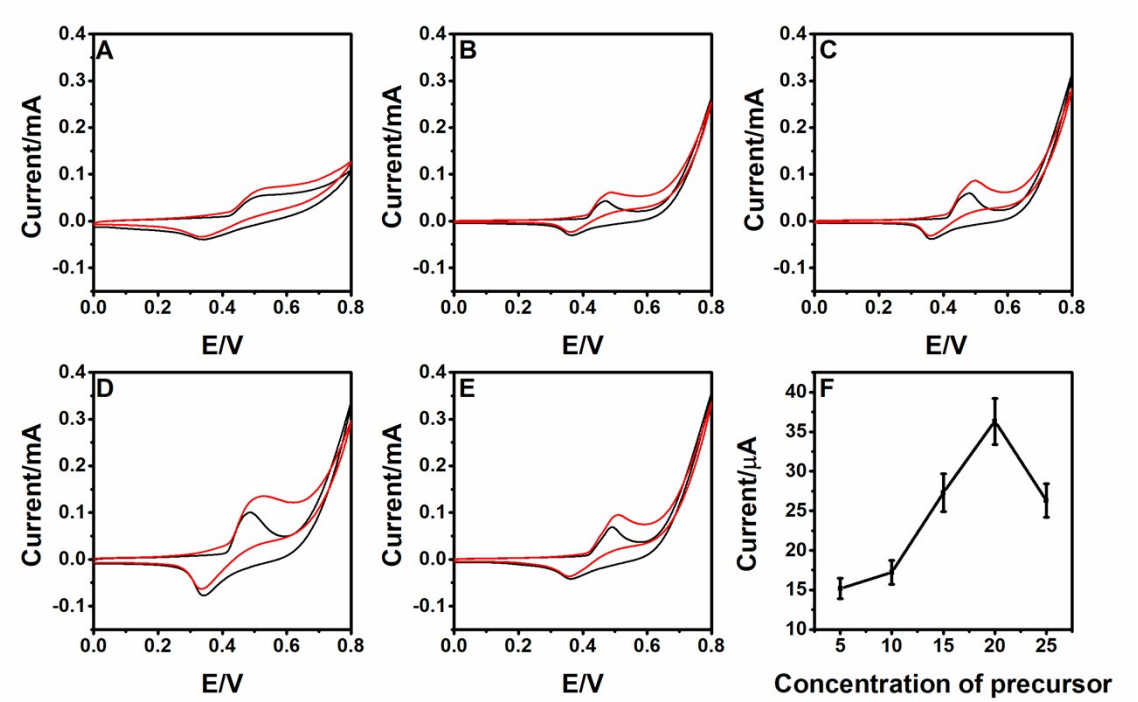

Figure S9 CV responses of Ni/3D GR at precursor concentration of (A) 5 mg mL^{-1}, (B) 10 mg mL^{-1}, (C) 15 mg mL^{-1}, (D) 20 mg mL^{-1} and (E) 25 mg mL^{-1} in the 0 (black line) and 2 (red line) mM glucose in 0.1 M NaOH. (F) The dependence of current response on the concentration of precursor.

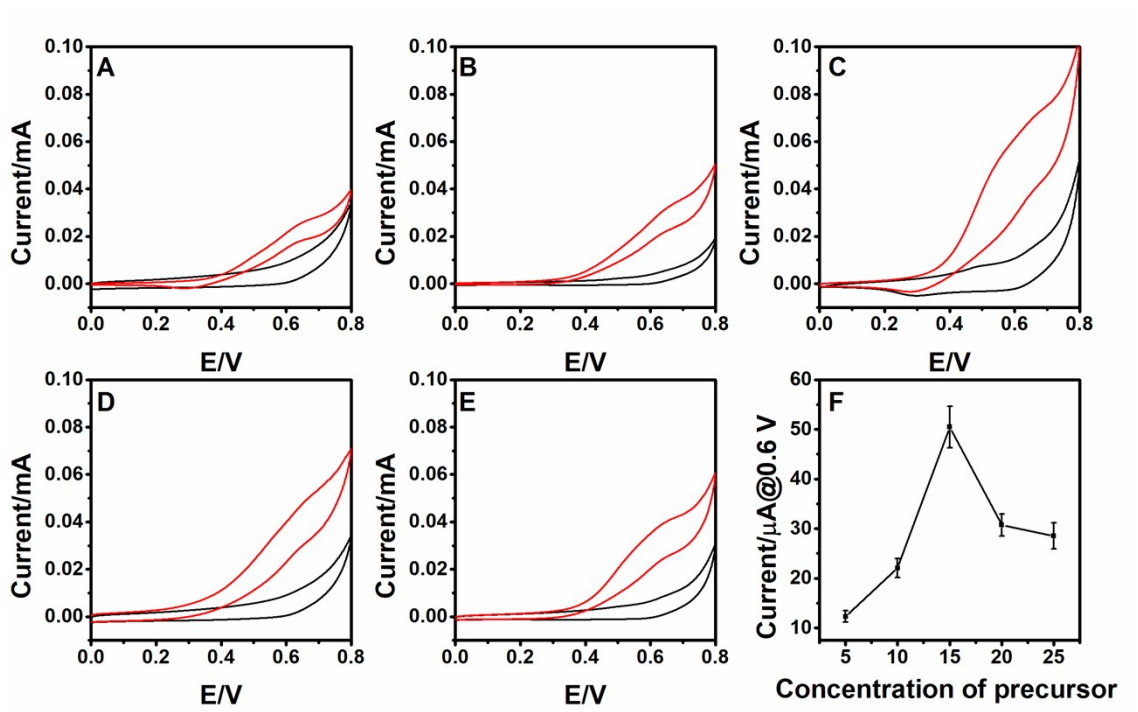

Figure S10 CV responses of Cu/3D GR at precursor concentration of (A) 5 mg mL^{-1}, (B) 10 mg mL^{-1}, (C) 15 mg mL^{-1}, (D) 20 mg mL^{-1} and (E) 25 mg mL^{-1} in the 0 (black line) and 2 (red line) mM glucose in 0.1 M NaOH. (F) The dependence of current response on the concentration of precursor.

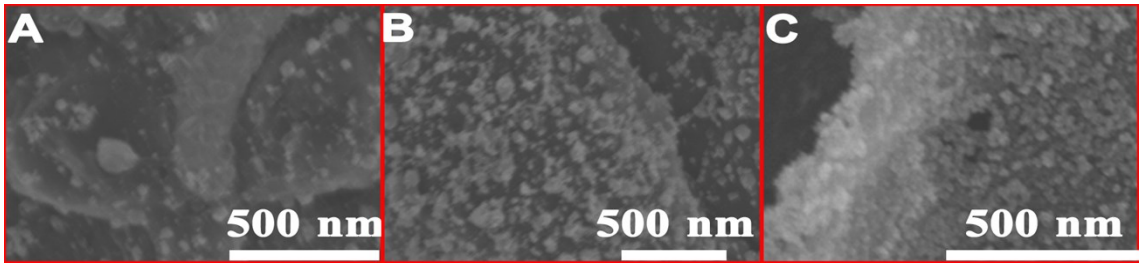

Figure S11 SEM images of Co/3D Gr at laser power of (A) 6 W, (B) 7 W and (C) 9 W.

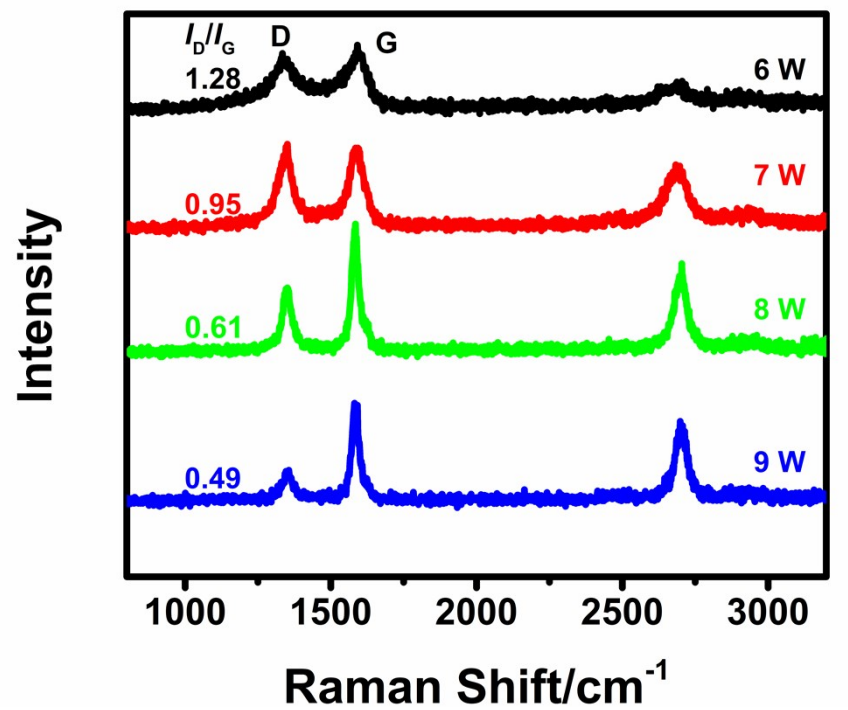

Figure S12 Raman spectra of Co/3D GR prepared at different laser power.

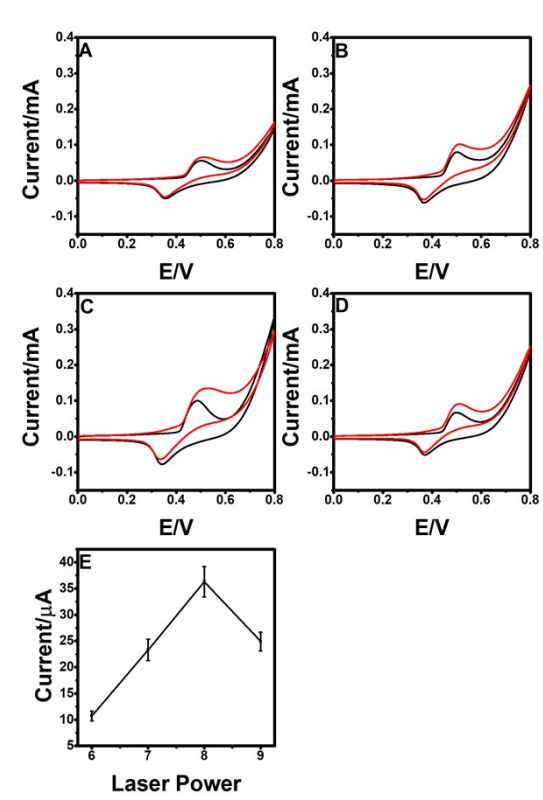

Figure S13 CV responses of Ni/3D GR at laser power of (A) 6 W, (B) 7 W (C) 8 W, (D) 9 W in the 0 (black line) and 2 (red line) mM glucose in 0.1 M NaOH. (E) The dependence of current response of Ni/3D GR on the laser power.

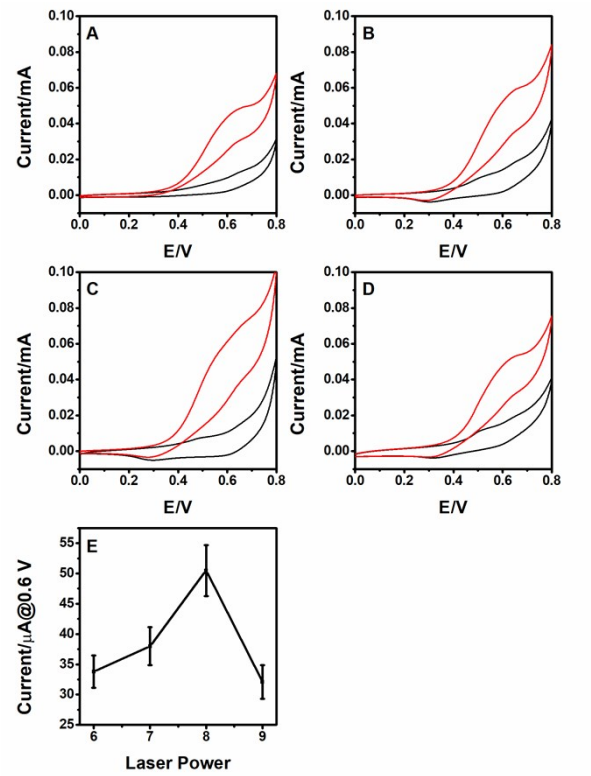

Figure S14 CV responses of Cu/3D GR at laser power of (A) 6 W, (B) 7 W (C) 8 W, (D) 9 W in the 0 (black line) and 2 (red line) mM glucose in 0.1 M NaOH. (E) The dependence of current response of Cu/3D GR on the laser power.

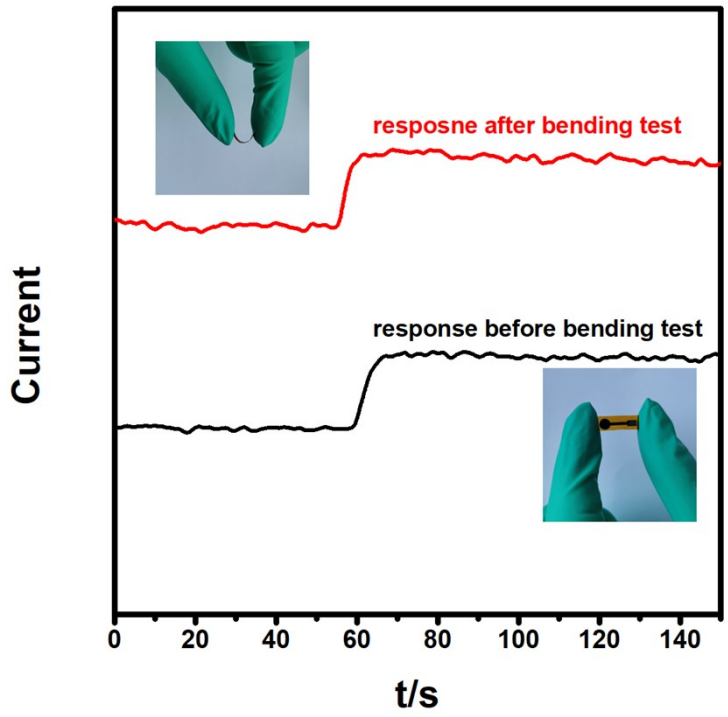

Figure S15 The electrochemical response before and after bending test.

Table S1 Comparison of preparative method and analytical performance of Co/3D GR with other MOFs-derived sensors.

Electrode	preparative method	Sensitivity (μA mM^{-1} cm^{-2})	Linear range (μM)	LOD (μM)	Reference
GR@ ZIF-67	In situ liquid-phase growth/ 3h/Air	1521.1	1-805.5	0.36	1
ZIF-N_2[a]	Thermal annealing/ 6h/700℃/N_2	227	100-1100	5.69	2
CoP/Co-BP[b]	Thermal annealing/2h/ 900℃/N_2	6427	0.5-1800	0.2	3
$NiCo_2O_4$ HNCs/GCE[c]	Thermal annealing/1h/350℃/ N_2	1306	0.18-5100	0.027	4
RGO-Co_3O_4[d]	Thermal annealing/3h/550℃/ N_2	1315	1-500	0.4	5
Co_3O_4/$NiCo_2O_4$ /CC[e]	Thermal annealing/2h/ 350℃/Air	12835	1-1127	0.64	6
Cuo NWs@ Co_3O_4	Thermal annealing/3h/ 350℃/Air	6082 μA $μM^{-1}$	0.5-100	0.23	7
Ag@ZIF-67	sequential deposition-reduction/12h/80℃/Air	379	2-1000	0.66	8
NiCo- MOF	Thermal annealing/4h/120℃/ N_2	684.4	1-8000	0.29	9
Co-MOF/NF[f]	Hydrothermal treatment/12h/125℃/ Air	10886	10-3000	0.001	10
3D- KSCs/ Co_3O_4[g]	Thermal annealing/4h/400℃/ N_2	1377.8	88-7000	26	11
3D/GR	Laser irradiation/air/room temperature	1411.2	10-3020	2.7	This work

a□ ZIF-N_2：pyrolysis of ZIF-67 under N_2 atmosphere.

b□ CoP/Co-BP: buckypaper decorated with CoP/Co.

c□ $NiCo_2O_4$HNCs/GCEHNCs/GCE: $NiCo_2O_4$ hollow nanocages modified glass carbon electrode.

d□ ZIF-67 derived Co_3O_4 anchored reduced graphene oxide sheets.

e□ Co_3O_4 hollow nanocubes on carbon cloth-supported $NiCo_2O_4$ nanowires.

f□ Co-MOF/NF: Co-MOF array on Ni foam.

g□ 3D-KSCs/hierarchical Co_3O_4:Three-dimensional kenaf stem-derived carbon/ hierarchical Co_3O_4

Table S2 Detection of glucose level in serum sample using Co/3D GR electrode.

Sample	Concentration by hospital determined by spectroscopic method (mM)	Concentration by sensor (mM)	Relative error	RSD% (n=3)
1	5.7	5.4	-5.5%	6.7
2	6.9	6.4	-7.2%	4.2
3	9.4	9.1	-3.3%	7.1

Reference

S1. Chen, X.; Liu, D.; Cao, G.; Tang, Y.; Wu, C., In Situ Synthesis of a Sandwich-like Graphene@ZIF-67 Heterostructure for Highly Sensitive Nonenzymatic Glucose Sensing in Human Serums. *ACS Appl. Mater. Interfaces* **2019,** *11* (9), 9374-9384.

S2. Shi, L.; Li, Y.; Cai, X.; Zhao, H.; Lan, M., ZIF-67 derived cobalt-based nanomaterials for electrocatalysis and nonenzymatic detection of glucose: Difference between the calcination atmosphere of nitrogen and air. *J. Electroanal. Chem.* **2017,** *799*, 512-518.

S3. Hou, C.; Zhang, X.; Wang, L.; Zhang, F.; Huang, X.; Wang, Z., A buckypaper decorated with CoP/Co for nonenzymatic amperometric sensing of glucose. *Microchim. Acta* **2020,** *187* (2), 101.

S4. Feng, Y.; Xiang, D.; Qiu, Y.; Li, L.; Li, Y.; Wu, K.; Zhu, L., MOF-Derived Spinel $NiCo_2O_4$ Hollow Nanocages for the Construction of Non-enzymatic Electrochemical Glucose Sensor. *Electroanalysis* **2020,** *32* (3), 571-580.

S5. Vilian, A. T. E.; Dinesh, B.; Rethinasabapathy, M.; Hwang, S.-K.; Jin, C.-S.; Huh, Y. S.; Han, Y.-K., Hexagonal Co_3O_4 anchored reduced graphene oxide sheets for high-performance supercapacitors and non-enzymatic glucose sensing. *J. Mater. Chem. A* **2018,** *6* (29), 14367-14379.

S6. Guo, Q.; Zeng, W.; Liu, S.; Li, Y., In situ formation of Co_3O_4 hollow nanocubes on carbon cloth-supported NiCo2O4 nanowires and their enhanced performance in non-enzymatic glucose sensing. *Nanotechnology* **2020,** *31* (26), 265501.

S7. Muthurasu, A.; Kim, H. Y., Fabrication of Hierarchically Structured MOF-Co_3O_4 on Well-aligned CuO Nanowire with an Enhanced Electrocatalytic Property. *Electroanalysis* **2019,** *31* (5), 966-974.

S8. Meng, W.; Wen, Y.; Dai, L.; He, Z.; Wang, L., A novel electrochemical sensor for glucose detection based on Ag@ZIF-67 nanocomposite. *Sens. Actuators, B* **2018,** *260*, 852-860.

S9. Li, W.; Lv, S.; Wang, Y.; Zhang, L.; Cui, X., Nanoporous gold induced vertically standing 2D NiCo bimetal-organic framework nanosheets for non-enzymatic glucose biosensing. *Sens. Actuators, B* **2019,** *281*, 652-658.

S10. Li, Y.; Xie, M.; Zhang, X.; Liu, Q.; Lin, D.; Xu, C.; Xie, F.; Sun, X., Co-MOF nanosheet array: A high-performance electrochemical sensor for non-enzymatic glucose detection. *Sens. Actuators, B* **2019,** *278*, 126-132.

S11. Wang, L.; Zhang, Y.; Xie, Y.; Yu, J.; Yang, H.; Miao, L.; Song, Y., Three-dimensional

macroporous carbon/hierarchical Co_3O_4 nanoclusters for nonenzymatic electrochemical glucose sensor. *Appl. Surf. Sci.* **2017,** *402*, 47-52.